Journal of Cleaner Production 469 (2024) 143111

Contents lists available at ScienceDirect

Journal of Cleaner Production

journal homepage: www.elsevier.com/locate/jclepro

Smart electroactive self-repairable coating involving end-of-life aircraft prepregs by mechanical recycling

Emma Espeute [a,*], David Martinez-Diaz [a], Pablo Vázquez Sánchez [b], Zulima Martín [b], Gilberto Del Rosario [c], Alberto Jiménez-Suárez [a], Silvia G. Prolongo [a,d,**]

[a] Materials Science and Engineering Area, Rey Juan Carlos University, Móstoles, Spain
[b] AIRBUS, P° John Lennon S/n, 28906, Getafe, Madrid, Spain
[c] Centro de Apoyo Tecnológico, Rey Juan Carlos University, Móstoles, Spain
[d] Instituto de Tecnologías para La Sostenibilidad, Rey Juan Carlos University, Móstoles, Spain

ARTICLE INFO

Handling Editor: Panos Seferlis

Keywords:
Recycling
CFRP
Coating
EoL prepreg
Joule heating
Self-healing

ABSTRACT

The environmental impact of the Carbon Fiber Reinforced Polymers (CFRPs) industry, particularly due to waste generation during manufacturing and end-of-life phases, is compelling major industrial entities to reconsider a circular economy approach for their materials and to comply with emerging regulations. This study explores the potential of recycled carbon fibers (rCFs) derived from the mechanical recycling of prepreg waste. Mechanical recycling was selected for its cost-effectiveness and moderate environmental impact, recovering short rCFs with lengths below 200 μm. These rCFs, which retain excellent electrical properties, are incorporated into an epoxy matrix with Polycaprolactone (PCL) to create a multifunctional coating with self-healing capabilities. The resulting composite material exhibited significant improvements in electrical conductivity, achieving up to 16.50 S/m, and demonstrated effective Joule effect heating, exceeding 200 °C with 20 V applied for a composite containing 15 wt% rCF. The self-healing efficiency for surface cracks, activated by the Joule effect, reached 80–90 %, resulting in a 99 % reduction in energy consumption compared to conventional oven heating. Notably, the self-healing mechanism was characterized in real-time within a scanning electron microscope for the first time, providing a comprehensive evaluation of the process. This innovative coating offers promising applications in aviation for anti-icing, deicing, and maintenance reduction, as well as in residential settings as an energy-efficient floor heating solution. This research underscores the potential of mechanically recycled CFRPs to produce high-value, sustainable materials, promoting a circular economy and reducing the environmental footprint of the aeronautical sector.

1. Introduction

A new industrial era has emerged in recent years, shaped by the consequences of climatic impacts and focusing on major industrial sectors (Moghaddam et al., 2018; Böhringer, 2003; Witik et al., 2013). Among these, the aeronautical sector is particularly affected by environmental damage due to its annual increase in usage, demand, and CO2 emissions (Chapman, 2007). According to Grossling et al., the number of aircraft in service is projected to increase by 88 percent between 2007 and 2027, from 19,000 to 35,800, to meet growing market demands. The aviation industry justifies this expansion with a 75 percent improvement in fuel efficiency over the past 40 years, largely due to the adoption of lightweight structures (Stefan and Paul, 2009). This weight reduction is primarily attributed to the increased use of Carbon Fiber Reinforced Polymers (CFRPs) as replacements for aluminum in primary and secondary structures (Wang and Duong, 2016).

However, with CFRPs comprising nearly half of new commercial aircraft models and the expected market growth, the industry faces significant manufacturing and environmental challenges; making CFRP usage a contentious issue with 90 percent of the environmental footprint related to the energy consumption for raw fabrication (Bianchi et al., 2021) (Pimenta and Pinho, 2011). This anticipated market expansion also raises concerns about waste management, incorporating concepts of prevention, recovery, reuse, and recycling (Gharfalkar et al., 2015).

* Corresponding author. Materials Science and Engineering Area, Rey Juan Carlos University, Móstoles, Spain.
** Corresponding author. Materials Science and Engineering Area, Rey Juan Carlos University, Móstoles, Spain.
E-mail addresses: emma.espeute@urjc.es (E. Espeute), silvia.gonzalez@urjc.es (S.G. Prolongo).

https://doi.org/10.1016/j.jclepro.2024.143111
Received 22 March 2024; Received in revised form 4 July 2024; Accepted 7 July 2024
Available online 10 July 2024

Despite the uncertainty surrounding the development of a second-generation CFRP market (Sommer and Walther, 2021), the lack of recycling alternatives in the near future is projected to result in a cumulative amount of End-of-Life (EoL) CFRP reaching 23,360 t/year by 2035 (Karuppannan et al., 2020), representing almost 12,000 EoL airplanes removed from service (Dayi et al., 2016).

The covalently cross-linked nature of these CFRPs, typically composed of thermosetting matrices, prevents them from being re-melted, re-processed, or reused (Chen et al., 2022; Martinez-Diaz et al., 2022), leaving landfilling (79%) and incineration (12%) as the predominant alternatives due to their low cost (Zhao et al., 2023; Vo Dong et al., 2018). These two options, leading to further environmental degradation and inefficient resource utilization, have prompted the development of new recycling methods. Current alternatives for separating Carbon Fibers (CFs) from the matrix include three major approaches, extensively analyzed in various studies (Zhang et al., 2020; Sukanto et al., 2021; Knappich et al., 2019; Lee et al., 2020; Lopez-et al., 2021); chemical methods (Solvolysis (Martinez-Diaz et al., 2022), Electrochemical, Microwave), thermal methods (Pyrolysis (Lopez-et al., 2021; Cheng et al., 2022), Fluidized bed), and mechanical methods (Milling (Shuaib and Mativenga, 2016), Grinding). The mechanical method has the lowest operational cost of recovery, consuming 0.27 MJ of energy compared to 30 MJ for Pyrolysis and 19.2 MJ/kg for solvent decomposition (Keith et al., 2016), and is also the least environmentally harmful alternative (Vo Dong et al., 2018). While there is no cost competition between landfilling, incineration, and recycling methods, recycled CFs offer a significant advantage for reuse. Developing recycling within the CFRP lifecycle could reduce production costs from less than $20/kg for virgin carbon fibers (vCFs) to $13–19/kg for second-generation CFs from thermo-chemical recycling (Vo Dong et al., 2018). A life cycle assessment (LCA) by A. Witik et al. revealed that using recycled CFs to replace vCFs could significantly reduce impacts on climate change (78%), resources (84%), and human health (65%) compared to landfilling (Witik et al., 2013), while proposing 50% material cost reduction (Hagnell and Åkermo, 2019). The application of mechanical recycling, as in this study, involves the recovery of short, recycled CFs (rCFs) (Li et al., 2016). These rCFs have recently been used in new applications, such as body panels for high-performance cars and commercial passenger vehicles (Bellam et al.). Additionally, recent research has focused on developing mechanical recycling of carbon fibers and their reuse in applications such as photocatalysis (Wu et al., 2023) and cement composites and concrete to improve compressive and flexural strength (Bhandari and Nam, 2024; Wang et al., 2023). Their morphology and properties are comparable to those of short carbon fibers (SCFs) synthesized by the industry. In similar applications, it has been demonstrated that incorporating SCFs (1–9 mm) at high content levels increases the electrical conductivity of cementitious composites (Ran et al., 2024). Their high electrical capacity also offers a significant advantage when combined with carbon nanotubes (CNTs) (Pal and Kumar, 2016) or graphene nanoplatelets (GNPs) (Saberi et al., 2023), resulting in a synergistic effect at both micro and nano scales as hybrid composites. Furthermore, the random distribution of SCFs has been shown to enhance electrical conductivity, even beyond the percolation threshold, elevating the electrical conductivity from 1 S/m to 2.2 S/m and 22.5 S/m with the incorporation of 5% and 10% SCFs, respectively (Pal and Kumar, 2016).

This specific investigation focuses on the mechanical recycling of CFRP manufacturing prepreg waste. Since the milling process alters the mechanical properties of CFs by reducing them from large to short fibers, the newly synthesized composites are produced as coatings. At the difference of the actuals research using rCFs as reinforcement, this study focuses on creating a value-added product in the form of a multifunctional coating. Developed by preserving the functionalities of rCF, such as thermal and electrical conductivity, this smart coating will include a new self-healing functionality by the incorporation of Polycaprolactone (PCL) into the thermoset matrix. Thanks to its properties the develop material will offer potential applications as the anti-icing and deicing activated by Joule effect. The current carbon fillers used for these applications can be classified in two groups: low voltages activation, as with the use of CNT achieving 150 °C with 25–100 V applied (Sangroniz et al., 2021; Sánchez-et al., 2022); and high voltage applied, as with GNP achieving 180–200 °C with 150–200 V applied (Sánchez-et al., 2020a) and more than 200 °C achieved with 10 V applied for SCFs (Zhao et al., 2022). Thus, this investigation is offering the development of an efficient self-healing by Joule effect through low voltage activation (under 100 V). Further investigations into coatings utilizing the Joule effect at low voltage application can be report, including the study by Xu et al., which reports achieving a temperature of 53.1 °C at 5 V for a 60 wt% SCF of 150 μm (Xu et al., 2023). Conversely, the application of 40V to a surface with 5 wt% GNP results in a temperature of 112.5 °C (Raji et al., 2016).

Due to the novelty of combining short rCFs with self-healing capabilities, a scarcity of related studies must be considered. The work by Sánchez-Romate et al. (Sánchez-et al., 2021) is a notable exception, linking electrical conductivity and self-healing through the Joule effect in an Epoxy/PCL/GNP system. The key findings from their study are presented in Table 1 for comparative analysis, along with additional research related to carbon-based reinforcement.

2. Experimental section

2.1. Materials

This study seeks to develop new intelligent multifunctional materials, in bulk and coating form. The fabrication of the material was obtained from the dispersion of short rCFs, manufactured through mechanical recycling of prepregs, in an epoxy matrix. The morphology of the material developed is a composite reinforced in short rCFs, discontinuous, randomly oriented and dispersed in a polymeric matrix. The rCFs came from an expired virgin prepreg roll and manufacturing cutting process from Automatic Tape Laying. The Bisphenol A diglycidyl ether (DGEBA) was chosen as the epoxy monomer, combined with a diamine hardener, the 4,4′diaminodiphenyl sulfone (DDS), both provided by Sigma-Aldrich. The Fig. 1 illustrates the cross-linking between the DGEBA and the DDS. A surfactant was selected, the Triton-X-100 purchased from Sigma-Aldrich, to improve the dispersion of rCFs in the non-cured DGEBA/DDS system. As a self-healing agent, the polycaprolactone (PCL) thermoplastic supplied by the same seller, was chosen to assure the self-reparation property of the material. Glass-fiber epoxy laminates Durostone EPC 203 provided by Röchling Composites was selected as the substrate for coating. In this study, all the chemicals received were used without further modification or purification.

2.2. Samples preparation

The manufacturing of the rCFs was realized through a mechanical milling process assured by a Universal Cutting Mill PULVERISETTE 19. To optimize the milling of the prepreg the maximum speed revolution of 3000 rpm was employed. This speed revolution was justified to prevent the accumulation of non-crushed prepreg in the mill and avoid material loss. Once incorporated into the machine, the pieces of prepregs were milled by a disk milling cutter rotor with fixed knives made of hard metal tungsten carbide, milling the prepreg into short fibers. These last ones were then passed through a recuperation sieve of 2 mm with trapezoidal perforation to be collected into a recovery box. The operation was repeated 10 times on each batch of prepreg to ensure uniform fiber size and reproducibility of the milling process.

To evaluate the effect of the rCF amount on the composite, different reinforcement contents were added, 5, 10, and 15 wt% of the final composite. These contents were selected such as lower quantities did not present noticeable changes in mechanical or electrical properties, and higher contents were considered unprocessable as measured in a

Table 1
State-of-the-Art of related investigations about Epoxy/Carbon-based reinforcement.

Filler Nature		Filler Length (μm)	Filler Amount (wt.%)	σ (S/m)	Ref.
CNT		10–30	2.0	7.50E−3	Chen et al. (2019)
			5.0	4.75E−2	Chen et al. (2019)
GNP		25	2.0	3.10E−4	Imran and Shivakumar (2018)
			8.0	4.00E−3	Prolongo et al. (2016)
GNP/PCL					
PCL Amount (wt.%)	*Self-healing Efficiency (%)*				
15	70	25	8.0	2.10E-1	Sánchez- et al. (2021)
20	58		8.0	2.35E−3	Sánchez- et al. (2021)
15	56		10.0	1.73	Sánchez- et al. (2021)
20	40		9.0	4.03	Sánchez- et al. (2021)
CB		20	40.0	1.40E−8	El- et al. (2002)
			70.0	1.00E−4	El- et al. (2002)
SCF		130	5.0	1.00E−5	Tsotra and Friedrich (2004)
		130	10.0	1.00E−4	Tsotra and Friedrich (2004)
		107	10.0	3.20E-10	Tsotra and Friedrich (2004)
		198	10.0	2.50E-7	Tsotra and Friedrich (2004)
		295	10.0	1.50E-4	Tsotra and Friedrich (2004)
		351	10.0	5.00E-3	Tsotra and Friedrich (2004)
rCF		200	5.0	5.40E−1	Martinez-Diaz et al. (2023)
			10.0	1.92	Martinez-Diaz et al. (2023)
			12.5	2.08	Martinez-Diaz et al. (2023)

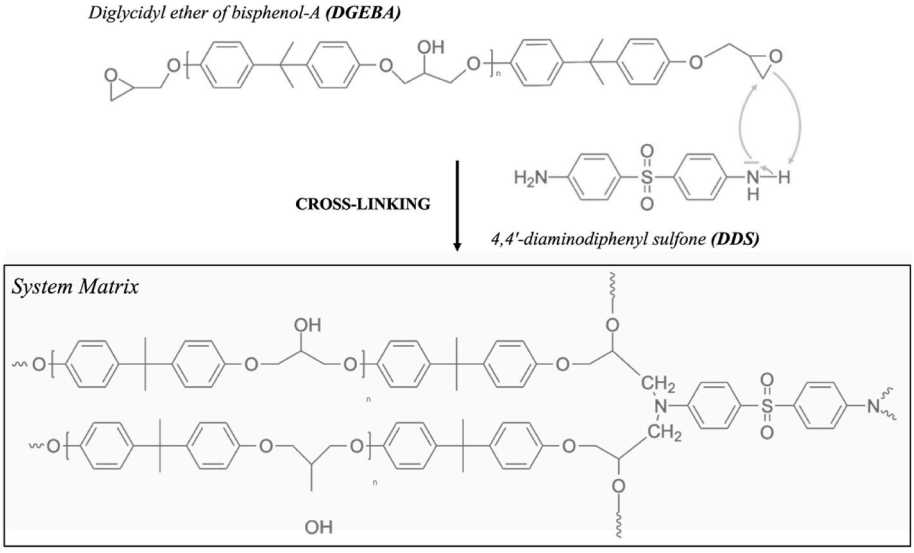

Fig. 1. Cross-linking between the DGEBA and the DDS

previous investigation (Martinez-Diaz et al., 2023). rCFs were incorporated under probe sonication into DGEBA with the Triton-X-100 for 15 min to ensure homogeneous mixing. The sonication process was applied with an ultrasound probe at a frequency of 24 kHz and a power of 400 W with a pulse amplitude of 50 % to improve the dispersion and with the assistance of a surfactant to prevent the formation of agglomerates. The mixture was then placed on a magnetic mixer at 100 °C to help the solution of the PCL inside of resin. The polycaprolactone is a thermoplastic component with a melting temperature of around 60 °C, therefore, to ensure a low viscosity of the PCL and facilitate its incorporation, the temperature was set at 100 °C. PCL content was referred to the epoxy resin, without taking the mass of the CFs into account. To evaluate the effect of the PCL in the final composite, different PCL amounts were added to the mixture: 5, 10, and 15 wt% of the matrix mass. Additionally, a sample without rCFs and with a 10 wt% of PCL was synthesized to be used as a reference in the self-healing characterization. Thus, the used conditions are summarized in Table 2.

The mixture was a first-time degassed by a vacuum pump to remove the air integrated during the ultrasound and the PCL addition, thus reducing the presence of residual porosity in the final materials. During this step, the temperature was kept constant. Finally, the DDS was incorporated in the following mass proportions DGEBA: DDS, 100:36.5 (stoichiometric ratio). Additionally, a second and final vacuum step was carried out.

The mixture was then poured into a mold to obtain bulk sample

Table 2
Summary of nomenclatures.

Nomenclature	rCF function of the final composite (%)	PCL function of the matrix mass (%)
C5P5	5	5
C5P10	5	10
C5P15	5	15
C10P5	10	5
C10P10	10	10
C10P15	10	15
C15P5	15	5
C15P10	15	10
C15P15	15	15
C0P10	0	10

material and on glass fiber epoxy laminates to obtain the coating samples. These last ones were done with the help of a doctor blade metal film applicator with a width of 100 mm and a 1 mm thickness gap at a constant speed of 1.5 mm s^{-1}. In both cases, the curing process of the samples was at 180 °C for 6 h in a convection oven. At this step, a treatment could be done directly on the bulk by performing a Joule heating of the material until reaching a temperature near the glass transition temperature (Tg). The origin of this last electrical treatment will be justified in the next section. According to the curing time and temperature selected, the curing degree of the final network was estimated to be close to 0.9, given a Tg around 188 °C (White et al., 2002) (Wang et al., 2023).

2.3. Characterization

2.3.1. Carbon fiber characterization

The length of the milled carbon fibers used in this study was characterized by optical microscopy image analysis, following the same protocol previously detailed elsewhere (Martinez-Diaz et al., 2023). Moreover, thermogravimetric analysis of the samples was carried out to evaluate the remaining original prepreg resin on the recycled fibers. Tests were performed using a heating rate of 10 °C.min^{-1} till 800 °C, in N_2.

2.3.2. Electrical conductivity characterization

A first measure of the electrical conductivity was realized with a Keithley-2410 source-meter instrument, at room temperature by the four-point probe method from 0 to 20 V for a limit current fixed to 1 A. A Joule effect treatment was effectuated between 0 to x V, x being the voltage required to reach a temperature near 150 °C for a limit current fixed to 3 A. To confirm the effectiveness of the treatment, a subsequent measurement of electrical conductivity is performed. An increase in electrical conductivity is observed between the first and subsequent measurements. The electrical conductivity of the samples was measured. In the case of a linear response of the current as a function of the voltage, the electrical conductivity (σ) values were evaluated by Ohm's law Eq. (1) The obtention of R from Eq. (1), i.e. the electric resistance of the sample expressed in Ohm (Ω), was used to determine the value of electrical conductivity (σ) Eq. (2) expressed in S.m^{-1}. Where A corresponds with the area of the cross-section (m^2) and it is correlated with thickness and width (t and l, respectively), i.e. the electron flow cross-section. L (m) is, as described before, the working distance between the electrodes.

$$I = \frac{V}{R} \tag{1}$$

$$\sigma = \frac{L}{R \cdot A} \tag{2}$$

The bulk samples were prepared with the following dimensions: 10x10 × 1 mm (L x l x e), while the coating samples were machined with the following ones: 18 × 18 mm as length (L) and width (l), while the thickness (t) corresponds to the one coating thickness done with the applicator: 1 mm.

2.3.3. Joule effect characterization

The evaluation of the Joule effect was done by using the same Keithley-2410 source meter instrument combined with a thermal camera (FLIR E50). Different voltages were applied to evaluate the reached temperature on the sample through the Joule effect, establishing a temperature limit of 150 °C to avoid the matrix degradation, as it has a Tg of around 188 °C (White et al., 2002). The Joule effect described in Eq. (3), results in a heat dissipation (Q) produced by the current flow (I) during a time (t) and the material's inherent resistance (R).

$$Q = I^2 \times R \times t \tag{3}$$

2.3.4. Self-healing characterization

To evaluate the self-healing capability of the different composites, the sample surface was analyzed, before and after a heat treatment, by optical profilometry and SEM. In this work the heat treatment (150 °C for 30 min) was performed in two ways, in a conventional oven, and by Joule effect, evaluating the principal differences of the two used methods. Additionally, the cross-sectional view of the sample was also analyzed, which allowed the evaluation of both the self-healing capability and the reinforcement distribution (PCL and rCF) of the samples.

Initially, three cracks of 150 μm deep were generated on the surface of the material by using a micrometer fitted with a blade that formed a 30° cutting edge, as visible in Fig. 2. The crack is produced by adjusting the z-axis zero point when the tip of the blade meets the sample surface. From this parameter, a penetration depth of 150 μm is adjusted by the machine. This protocol ensures the perfect reproducibility of the method. The crack volume was measured with a Zeta Z-20 optical profilometer before (V_0) and after (V_1) the heat treatment to evaluate the self-healing reparation ratio by comparing 15 different areas and using the Mountains software from Digital Surf. The application of the following Eq. (4) gives the self-healing efficiency (SH):

$$SH(\%) = \frac{V_0 - V_1}{V_0} \times 100 \tag{4}$$

The presented results of self-healing tests are given as an average of the results obtained for the 3 cracks made on the surface of each sample. Moreover, the self-healing capabilities of the developed composites were also analyzed in real-time by using a SEM (Prisma E, tungsten filament), with the ability to raise the temperature inside the chamber reaching more than 200 °C for a magnification of 150×. The 0.5 mm-diameter samples used in this evaluation are obtained straight from the manufactured coatings. This method allowed to illustrate the phenomenon of self-healing as it was recorded in live mode the process.

2.3.5. Energy consumption characterization

A study was performed to evaluate the energy consumption between the self-healing performed in the oven and by the Joule effect. Eq. (5) was used to evaluate the power (P) generated during the Joule heating. On the other hand, Eq. (6) was applied directly to calculate the consumption (E) expressed in (KWh) during the self-healing, knowing in advance the power (P) in kilowatts (KW) of the oven model and the duration (t) in hours (h) of the treatment.

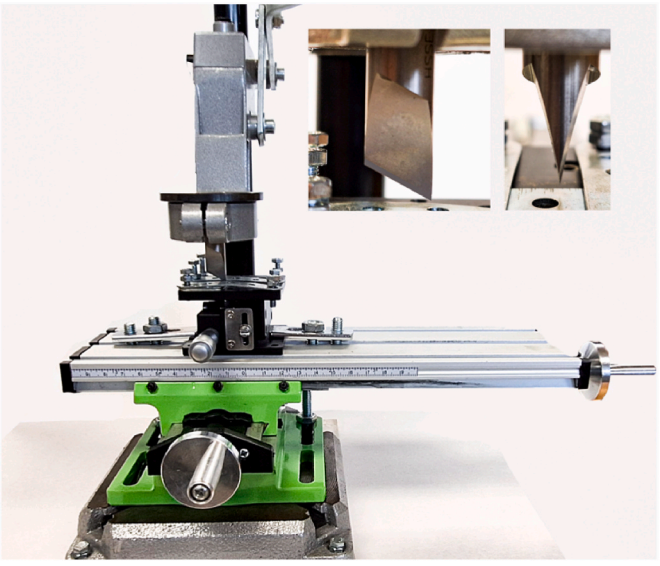

Fig. 2. Micrometer used for crack generation.

$$P(W) = U(V) \cdot I(A) \quad (5)$$

$$E(KWh) = P(KW) \cdot t(h) \quad (6)$$

The oven used was a Kendro Laboratory product, Type UT 6 with a general power of 1.27 KW.

3. Results and discussion

3.1. Recycled carbon fiber characterization

The mechanical recycling procedure underwent optimization aimed at minimizing residual prepreg matrix and fiber dimensions. Experimental evidence illustrated that subjecting the material to 10 cycles of milling yielded a homogeneous polydispersity among carbon fibers (Fig. 3c), facilitating the attainment of processable fiber lengths while concurrently eliminating unprocessed prepreg remnants from prior cycles (Fig. 3a) and b). According to the polydispersity results obtained on more than 250 specimens from optical microscopy analysis, 70 % of the measured rCFs have a length lower than 200 μm (Bhandari and Nam, 2024) (Fig. 4a). This milling regimen effectively contributed to mitigating the prevalence of the original prepreg resin. The presence of residual original resin surrounding individual carbon fibers can markedly compromise the performance characteristics of the resultant composite synthesized which could be the result of a deficient interfacial adhesion between the rCFs and the new matrix DGEBA/DDS. Furthermore, the electrically insulating nature of residual original prepreg resin poses a risk of diminishing the electrical conductivity of the recycled composite. Consequently, minimizing the residual prepreg resin content emerges as a critical prerequisite for achieving enhanced integration of rCFs within the new matrix as demonstrated in a previous investigation involving 10 cycles of milling (Martinez-Diaz et al., 2023).

A TGA was performed to determine the amount of remaining expired epoxy resin on the prepreg before and after the mechanical recycling process. As a result, it can be concluded that the milling process reduces the original prepreg resin of the final product by around 10 %, as can be observed from the TGA result in Fig. 4b. Additionally, Table 3 summarizes more information about the TGA analysis, such as the mass variations in percent according to ranges of temperature, beginning of loss (T onset), and end of loss (T offset). The degradation temperature of the matrix is around 395 °C for both materials (Fig. 4b). As previously commented, the milling process contributes to the partial removal of the original prepreg resin from the rCF surfaces. This removal generates a mixture of rCFs with and without free residual original resin. The TGA of the fibers from the prepreg (CF Original Prepreg without milling) reveals a mass variation of 21.6 % between 364 °C and 433 °C while the mass loss is 14.2 % for the rCFs. Considering that the sample analyzed was representative of this mixture of resin and rCFs, it can therefore be estimated that the milling provides a minimum of 7.4 % resin removal.

3.2. Electrical conductivity

During the electrical conductivity tests, a phenomenon was observed that led to an increase in the electrical conductivity for all samples, after an initial voltage was applied. Due to the Joule effect heating generated in each sample when applying a different voltage during the electrical conductivity tests, it was observed that the conductivity increased when performing a second measurement on those samples that reached a temperature close to the matrix Tg during the first test. Furthermore, this increase in conductivity persisted over time, meaning that no subsequent decrease in electrical conductivity was observed in any case. To analyze in detail the influence of this Joule effect treatment on the electrical conductivity, a particular composition was selected to allow a precise comparison: C15P10, the higher percentage of carbon fibers to ensure the best electrical conductivity, combined with the midpoint of PCL contents. In this case, the electrical conductivity of the sample was 0.82 S m^{-1} before reaching a temperature close to the Tg on the sample, and 13.7 S m^{-1} before heating the sample by Joule effect near to the Tg, representing this time an increase of more than 1680 %. This electrical conductivity increase was not observed when the samples were heated up to the Tg using a conventional oven.

The first hypothesis was that the original prepreg resin still surrounded the rCFs after milling, adversely affecting conductivity. By producing a Joule effect treatment, increasing the temperature above the Tg can degrade the original prepreg matrix. This degradation can increase electrical conductivity by removing the insulating resin layer. Electrical conductivity is influenced by temperature, and the Arrhenius equation links temperature to electrical conductivity exponentially (Eq. (7)). According to this equation, the electrical conductivity of composites should rise with temperature, mobility (μ_n and μ_p), and electron jump distance, which is known to improve electrical conductivity (Polymer Blend Nanocomposites for Energy, 2023).

$$\sigma = n_0 q \left(\mu_n + \mu_p\right) exp\left(\frac{-E_g}{2k_B T}\right) \quad (7)$$

However, the Joule effect treatment induces a permanent increase in electrical conductivity, even at room temperature and low voltages, which doesn't follow Eq. (7). This could be due to a permanent change in μ_n and μ_p), or increased chain mobility near Tg, creating a preferential conductivity pathway. TGA results show resin degradation begins around 367 °C for the original prepreg resin and 382 °C for the new DGEBA/DDS matrix (Fig. 4b). This improvement aligns with the Negative Temperature Coefficient of Resistivity effect (NTCR), where resistivity decreases as temperature increases. NTCR involves hypotheses about Tg, particle migration, and conductive paths (Taherian and

a) **b)** **c)**

Fig. 3. Morphology of prepreg during milling for 2 cycles **(a)**, 5 cycles **(b)** and 10 cycles **(c)**.

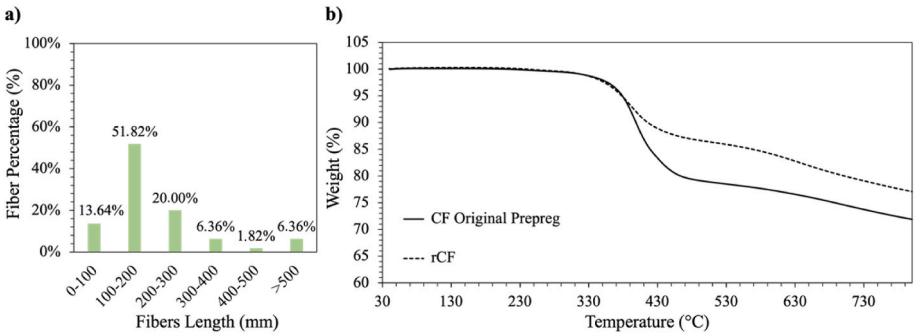

Fig. 4. Polydispersity analysis of the recycled carbon fibers **(a)** TGA analysis of the used prepreg carbon fibers before and after the milling process **(b).**

Table 3
TGA data related to the fibers.

	Step	Weight loss (%)	T (onset °C)	T (inflection °C)	T (offset °C)
CF Original Prepreg	1	21.65	363.76	397.89	432.86
	2	11.12	620.29	694.16	–
rCF	1	14.27	343.90	391.51	428.03
	2	9.61	576.15	639.03	–

Ghorbani, 2017). Finally, a second hypothesis can be elucidated as a nanometric modification of carbon fiber surfaces that could explain this irreversible behavior. The Joule effect process could modify the microstructure of the composite. The authors of this hypothesis concluded that a structural modification of the carbon fiber was occurring with the increase of the current, involving an identical d-spacing and crystal size but with a higher orientation (Taherian and Ghorbani, 2017).

Fig. 5 shows the electrical conductivity measured after Joule effect treatment. Two different variables were analyzed, the rCF and PCL contents. The selection of the contents was based on two criteria: firstly, increasing the amount of rCF beyond 15 wt% resulted in a mixture with poor dispersion and high viscosity, making it very difficult to process. On the other hand, concerning the PCL amount, literature indicated that percentages close to 20 wt% have negative effects on the self-healing capabilities of the DGEBA/DDS system (Jiménez-Suárez et al., 2020), which was one of the main objectives of the present work.

As can be observed in Fig. 5, an increase in the rCF amount results in an augmentation of the final electrical conductivity. However, this behavior is not linear for any of the three different PCL percentages studied. With a low rCF content, doubling the amount of reinforcement from 5 to 10 wt% results in doubling the electrical conductivity of the samples, on the other hand, increasing the rCF content by another 5 wt% (from C10 to C15) leads to an average increase of 800 %, being slightly

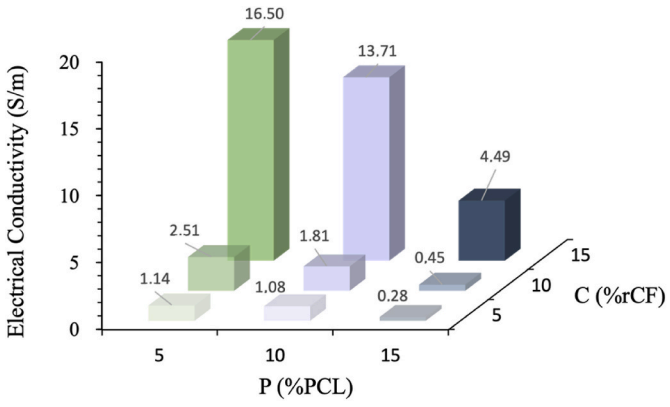

Fig. 5. Electrical conductivity of the composites as a function of rCF and PCL contents.

higher when the PCL content is higher (reaching a 1000 % increase). In summary, it can be concluded that a higher electrical conductivity increment occurs between 10 and 15 wt% rCF for all the PCL percentages considered.

In any case, it is noticeable that the introduction of PCL on the composite has a relevant influence in reducing the final electrical conductivity. In a similar way to the previously concluded for the rCFs, the effect of the PCL neither presents a linear trend with the content. The electrical conductivity drop associated with an increase in PCL from 10 to 15 wt% is significantly higher than the obtained one for the increase from 5 to 10 wt%, with a drop in the electrical conductivity of 74 and 17 %, respectively. This behavior has already been measured in similar research (Sánchez-et al., 2020b). The incorporation mechanism of PCL involves the miscibility of the thermoplastic with the matrix at high temperatures, followed by phase separation at lower temperatures, resulting in a dispersion of small particles due to the loss of miscibility. During this second step of curing, the rCFs tend to remain in the epoxy phase. However, at high filler concentrations, electrical pathways are limited and a small fraction of rCFs may partially penetrate the PCL particles, leading to a reduction in electrical conductivity due to the insulating nature of the thermoplastic.

Compared to the literature summarized in Table 1, the results obtained with rCFs, regardless of the fiber percentage, exhibit superior electrical conductivity values compared to those of Carbon Nanotubes (CNTs), Graphite Nanoplatelets (GNPs), Carbon Black (CB), and even Carbon Fibers (CFs). Specifically, for CFs, a 10.0 wt% filler amount with a similar length of 198 μm exhibits an electrical conductivity differential of seven orders of magnitude. This discrepancy can be attributed to the inherent differences between CFs and rCFs and protocol of introduction in the matrix. Additionally, a smaller difference in electrical conductivity is noted respected to the rCFs when compared to a previous work (Martinez-Diaz et al., 2023), using the same recycling source and milling protocol as this study. This minor variance in electrical conductivity may be explained by differences in the matrix systems, which affect the dispersion of rCFs due to variations in viscosity or even the insulating properties of the DGEBA/DDS and LY/XB systems. In conclusion, compared to the existing state-of-art, the rCFs produced and their incorporation into this specific epoxy matrix achieve some of the highest electrical conductivity results reported.

3.3. *Joule effect heating capability*

As a parallel effect to electrical conductivity, the Joule effect heating appears as a result of the loss of energy in the form of heat (Eq. (3)). In this study, the heating capability of the material was essential to assist self-healing without the necessity to use a conventional heating source. In a similar way to the electrical conductivity test, the Joule effect capability was also evaluated from 5 to 20 V, knowing in advance that the Joule effect of certain compositions was relatively fast. Moreover, taking the Tg of the composites and the melt temperature of the PCL into account, the temperature limit of the experiments was fixed at 150 °C,

an efficient temperature to ensure the right flow of the self-healing agent thanks to its low viscosity (Jiménez-Suárez et al., 2020) (Sánchez-et al., 2021).

To evaluate the effect of the rCFs and PCL amounts on the Joule effect heating capability, the achieved composite temperature at 20 V after 2 min is summarized in Fig. 6a. The composites of C15 are the ones that heat the most, in a more homogeneous form when the PCL content is low. The augmentation of PCL involves a delayed warm-up, a phenomenon visible in the samples of C5 in Fig. 6a.

After analyzing these results and taking the main objective of this work into account, the selection of the best material is taken based on rapid heating to a target temperature of 150 °C to generate a self-healing combined with a low voltage application to reduce energy consumption. So, in this way, the evolution of the achieved temperature as a function of the applied voltage and the PCL content is represented in Fig. 6b for the composites of C15, selected as the best option. It can be observed that the target temperature (150 °C), can be reached for the three composites, regardless of the PCL content.

3.4. Self-healing capability

The analysis of self-healing capability was only evaluated on the composites of C15 for the diverse evaluated PCL contents. Results of self-healing after analysis with the profilometer are represented in Fig. 7a. It can be observed that for both types of heating the increase of self-heating is function of the increase of the PCL amount. Firstly, when the lowest percentage of PCL is used, average repairs of 46 % are achieved with both heat sources. In addition, doubling the amount of PCL outcomes effectively doubles the healing capability, with average values ranging from 82 to 91% (from C15P5 to C15P10). Finally, increasing the amount of PCL by another 5 wt% (C15P15) does not contribute to an increase in repair capability, with a result that remains in the range of 81–90 %. In conclusion, the conditions C15P10 and C15P15 generate the same percentage range for self-healing for respected 10 % and 15 % PCL. This observation can be taken as the highest reparable range achievable. Contrary to the C15P5, the percentage of self-healing is not related with a lack of self-healing agent but may be justified by a loss of material during crack creation. This material loss cannot be regenerated; therefore, the percentage of repair is limited. Because of the latter, the material C15P10 is considered the best result. An example of profilometer mapping of a crack before and after self-healing by the Joule effect of this same composition is shown in Fig. 7b, the repair volume is obtained through the profilometer profile as illustrated in Fig. 7c. This conclusion is based on achieving a high healing capability, similar to the one obtained with the C15P15, while simultaneously achieving a 300 % higher electrical conductivity (13.7 S m^{-1} instead of 4.5 S m^{-1}). Moreover, due to the use of a smaller amount of PCL, the heating by the Joule effect is faster and more homogeneous, as shown previously in Fig. 6. This can be considered a significant advantage in terms of repair efficiency and energy consumption when the repair treatment is performed by using the Joule effect.

On the other hand, analyzing the efficiency of the heat source, similar results are obtained in both cases. Despite the observed differences, all the results fall within the measurement deviation, it can be so concluded that there is no significant difference in the outcome based on the heat source used for the repair treatment.

To analyze in detail what occurs in the reparation process, the cross-sectional view of the composite considered as the best result (C15P10) was observed before and after the repair process by FEGSEM. Fig. 8 collects the captured images where it can be observed that the generated cracks are not only filled with the thermoplastic material but also with the thermoset matrix and the rCF reinforcement. Both sides of the crack come together slightly, and it can be observed how some carbon fibers used as reinforcement move toward the interior of the crack (Fig. 8b).

To evaluate the repair mechanism, it was decided to analyze the repair process in real-time, instead of the before-and-after approach used so far. For this purpose, the repair process was conducted inside the SEM (Prisma E, tungsten filament) while recording the entire process on **video 1** and **video 2** (summarizing the obtained results in Figs. 9 and 10 respectively). After the crack generation, the samples were placed on the SEM and heated using a ramp temperature of 6 °C/min, with a minute of stabilization each 50 °C until 270 °C. Additionally, to evaluate if the rCFs could modify the repair mechanism, two materials with the same PCL amount but diverse percent of rCF were analyzed, C0P10 and C15P10.

Supplementary video related to this article can be found at https://doi.org/10.1016/j.jclepro.2024.143111

The live repair analysis allows the comprehension of the self-healing mechanism, where the property of thermal expansion of the PCL involves a Differential Expansive Blending (DEB) inside of the matrix. A phenomenon visible for both samples in SEM analysis (Figs. 9 and 10) where the thermoplastic flow to the surface even dragging away the rCFs used as reinforcement (as previously suggested in Fig. 8). The DEB appears at different times depending on the presence of rCFs. Without rCF the DEB appears at 28 min (Fig. 9c), in contrast with the case of using rCF as reinforcement where the DEB appears 10 min later (Fig. 10f). The presence of the DEB phenomenon can be visually correlated in the

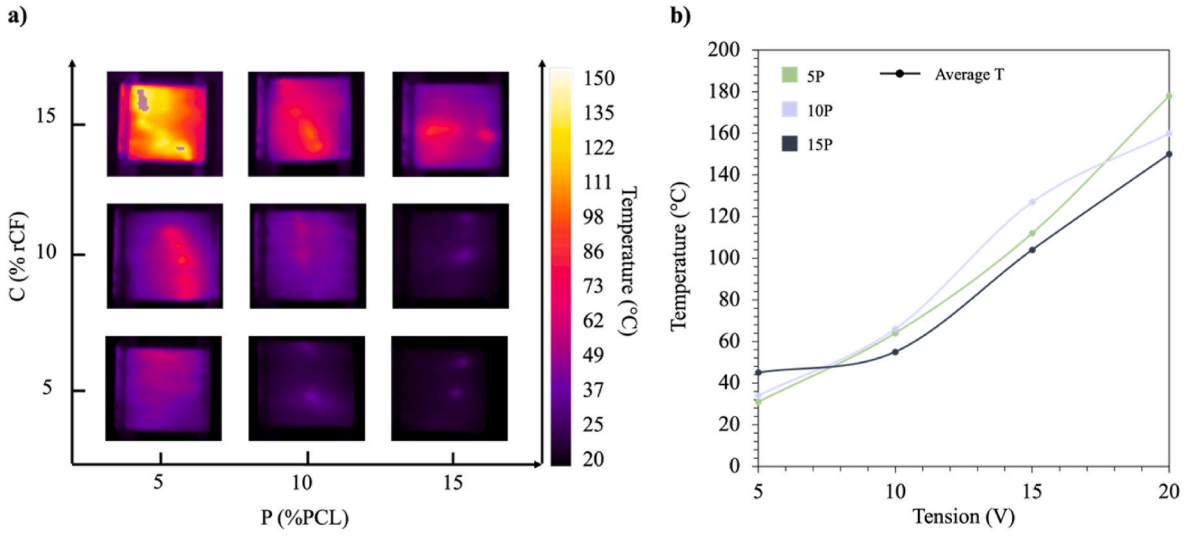

Fig. 6. Mapping of the achieved temperature by Joule effect with 20V in 2 min for all the compositions **(a)** and graphical representation of the Joule effect in function of the voltage applied (5–20) V for the samples C15 **(b)**.

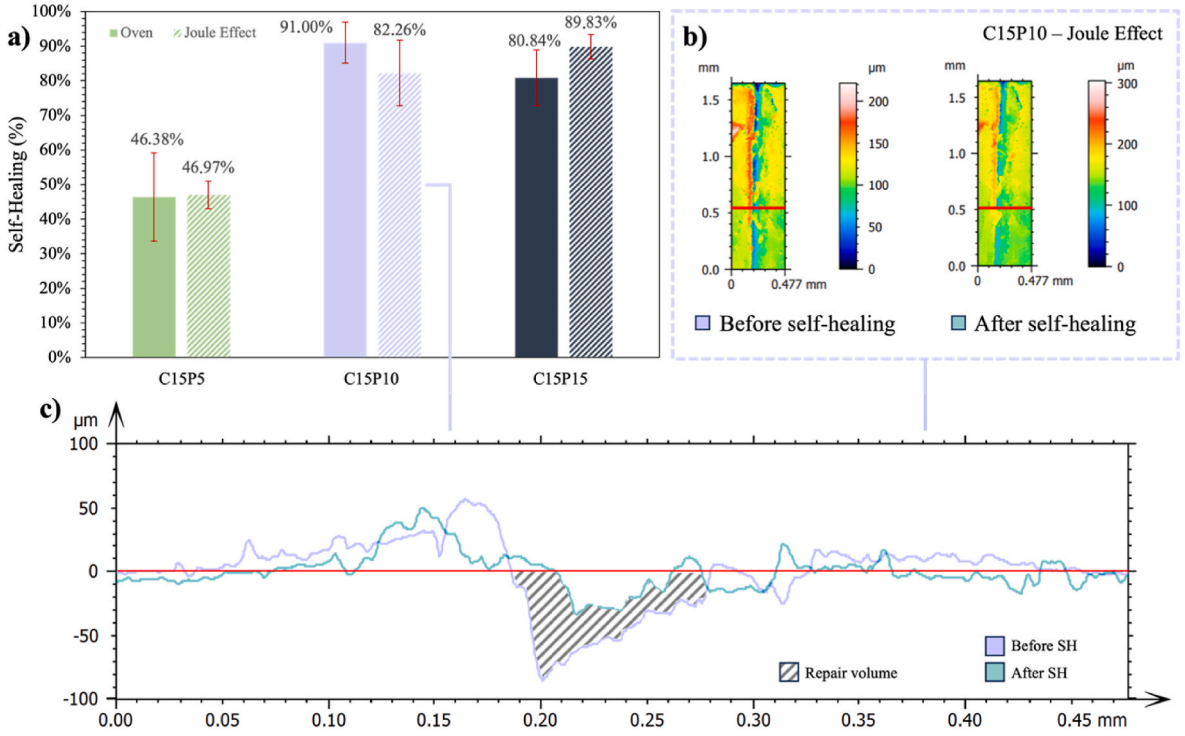

Fig. 7. Self-healing comparison on the samples of C15P(5; 10; 15) between heat generated by the oven and Joule effect **(a)**. Profilometer mapping **(b)** and profilometer profile **(c)** of a crack before and after self-healing on the composition C15P10 by Joule effect.

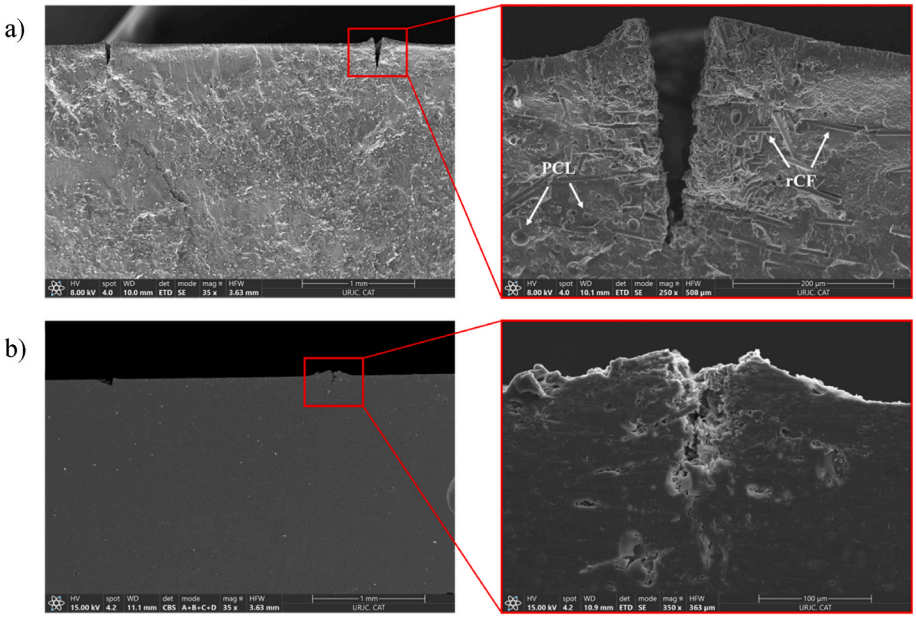

Fig. 8. FEGSEM images of the sample C15P10 before self-healing **(a)** and after self-healing by Joule effect **(b)**.

images with the appearance of what seem to be spheres on the surface. This modification made on the surface is not permanent, as it can be observed in both cases how it disappears subsequently between 40 and 50 min (Figs. 9g and 10g). However, its appearance does beneficially contribute to the mechanism of closing the generated cracks. The DEB results in a volumetric expansion difference between the PCL and the matrix, generating a large transient pressure on the PCL which is then in its liquid state (Luo et al., 2010). This mechanism is a behavior well-known for materials of self-healing using PCL due to its small compressibility and large liquid extensivity, contributing in this way to self-repairing (Luo et al., 2009). The PCL appeared faster on the surface in the sample without carbon fiber which confirms that the rCFs have an influence, impeding the self-healing. Moreover, analyzing the final self-healing result provided in Figs. 9 and 10, the presence of 15 wt% rCF on the material only reduces the self-healing efficiency by 5 %.

Finally, another conclusion that can be drawn from the characterization standpoint is that the self-repair values calculated from the analysis using SEM and profilometry are similar, around 80 %. A relevant observation as it validates the results previously obtained through profilometry, which is a much faster and cost-effective technique.

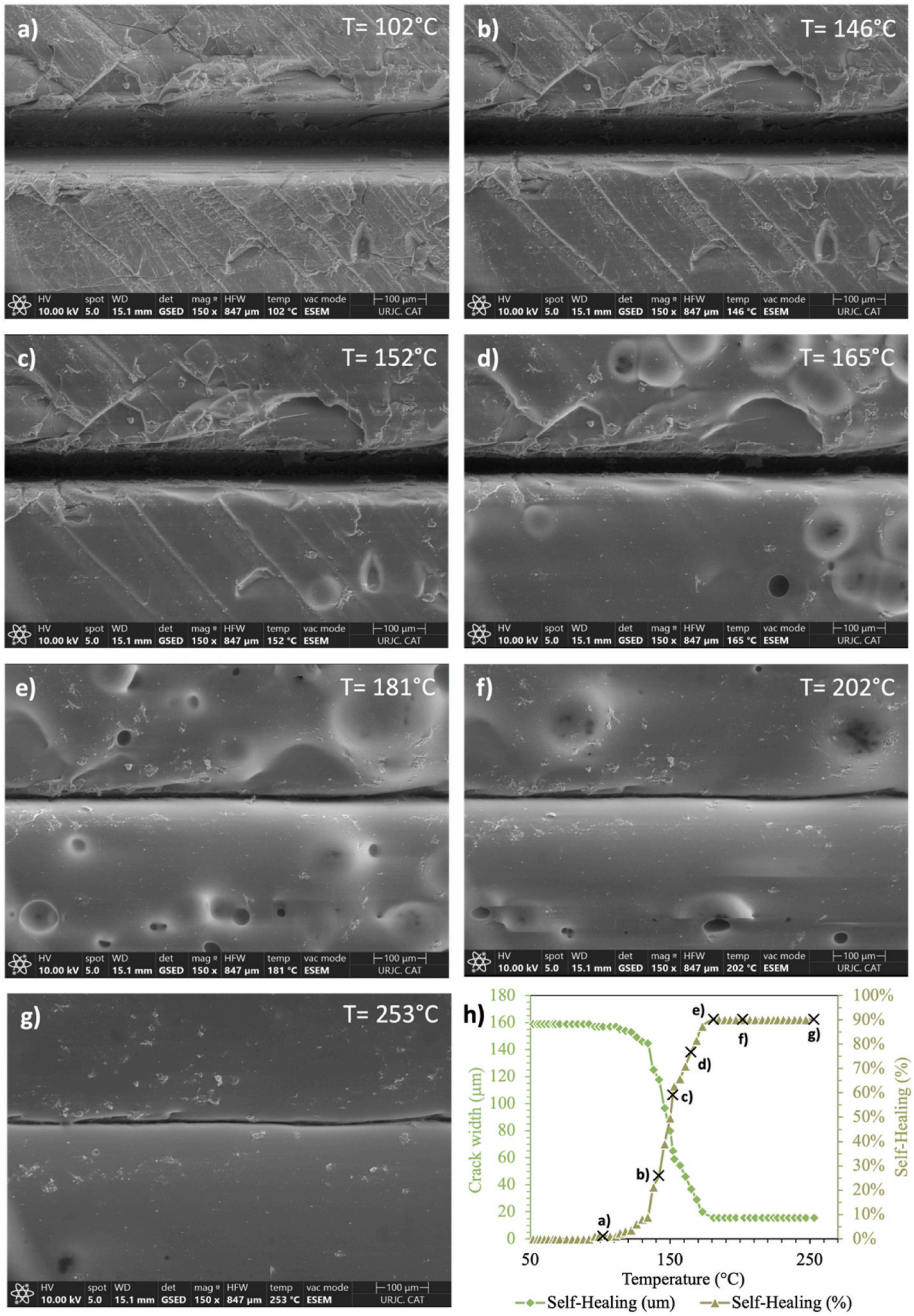

Fig. 9. Self-healing of the sample C0P10 generated in a FEGSEM, images representation **(a–g)**, and self-healing result evolution **(h)** in function of the temperature.

Moreover, it is important to note that, since the goal is to characterize the repair capability of different composites, cracks are created on the surface of the samples. It must be pointed out that the generation of these surface cracks involves material loss (Fig. 8), making it challenging to achieve 100 % repair.

Compared to the literature summarized in Table 4, the introduction of PCL in the form of microcapsules, dispersed as particles, proves to be the most efficient form. Although electrophoretic deposition requires a smaller amount of self-healing agent, potentially resulting in a minor impact on electrical conductivity, this technique is more applicable to continuous CFs. Regarding the nature of the fibers, rCFs exhibit superior performance in combination with PCL, showing an increase of approximately 20 % in self-healing for 15 wt%PCL with GNP compared to the P15C15 condition. Regarding the self-healing mechanism activated by the Joule effect, a significant reduction in the required voltage and an enhancement in self-healing efficiency should be noted. Specifically, there is a 20% increase in self-healing efficiency, improving from 70% to 90%, alongside a 93% reduction in activation voltage, decreasing from 300 V to 20 V.

3.5. Energy consumption of the different self-healing methodology

As previously concluded, the repair degree is similar instead of the used heating source (oven or Joule effect). Nevertheless, due to the inherent nature of each type of heating source, it is expected that the final energy consumption associated with a repair cycle will be different.

The profile of heating in the oven began with a ramp temperature of 10 min from 25 °C to 150 °C, followed by an isotherm of 150 °C for 30 min. The dimensions of the oven allowed the self-healing of the three specimens at the same time. In this way, the final energy consumption given by Eq. (6) is divided by 3 to determine the associated consumption with a single sample. On the other hand, the self-healing by joule effect

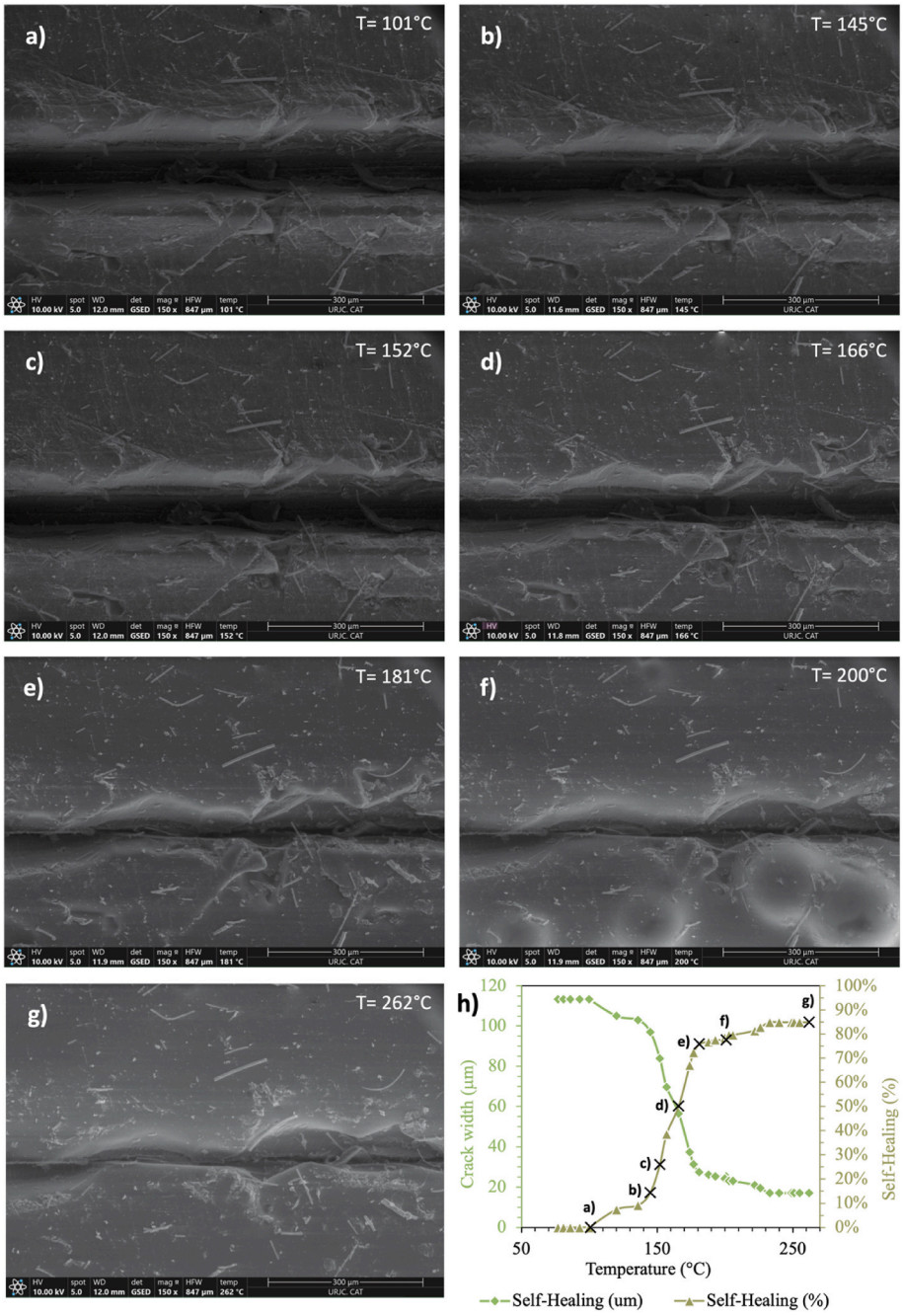

Fig. 10. Self-healing of the sample C15P10 generated in a FEGSEM, images representation **(a–g)**, and self-healing result evolution **(h)** in function of the temperature.

was characterized by a temperature ramp until 150 °C, followed by a 30-min dwell, at a specific voltage for each sample composition and an intensity that varies depending on the electrical conductivity of the material being analyzed. So, with this heating source, the final energy consumption given by Eq. (5) and Eq. (6) varies with each sample type, unlike what happened in the previous source. In this case, due to the used equipment, it is only possible to perform the self-heating of one sample at a time with this heating method. Table 5 summarizes the estimated energy consumption of the diverse heating sources and composites. As expected, the energy consumption coming from the heating done in the oven is much higher than that generated by the Joule effect. So, despite a similar reparation degree being obtained in both cases, the use of the joule effect heating implies lower energy consumption, along with the benefit of having no limitations on the size of the piece to be repaired, as well as the ability to perform in-service reparations. It is important to highlight that bigger structures would require bigger ovens while the Joule effect heating can be done selectively in one small area, being even more significant the differences between methods.

4. Conclusions

This investigation proposes the synthesis of an innovative environmentally friendly coating by mechanically recycling prepreg waste, characterized by low energy consumption and reduced CO_2 emissions, alongside the deliberate development of a more sustainable, self-powered material.

Demonstrating the potential to create high-value recycled carbon fiber products, these recycled fibers were used to synthesize a new multifunctional material reinforced with mechanically recycled carbon

Table 4
State-of-the-Art in Self-healing of Epoxy Matrix in function of the nature, form of incorporation and amount of agent.

System	Self-healing Agent	Agent incorporation form	Agent Amount (wt. %)	Self-healing efficiency (%)	Self-healing Mechanism	Ref.
Epoxy/glass composites	PCL	Electrophoretic Deposition	0.03	50	1 h at 80 °C	Simonini et al. (2023)
Epoxy/GNP composites	PCL	Microcapsules	15	70	100 °C (300 V)	Sánchez- et al. (2021)
			20	58	100 °C (250 V)	Sánchez- et al. (2021)
			15	56	100 °C (200 V)	Sánchez- et al. (2021)
			20	40	100 °C (100 V)	Sánchez- et al. (2021)
Epoxy/rCF coating	PCL	Microcapsules	5	47	30 min at 150 °C	P5C15
			10	82		P10c15
			15	90		P15C15

Table 5
Energy consumption in function of the heating source and of the amount of PCL for specimens C15.

	PCL content		
	5 %	10 %	15 %
Oven Heating (KWh)	1.7639	1.7639	1.7639
Joule Effect (KWh)	0.0126	0.0132	0.0158
Reduction of energy consumption (%) [a]	99	99	99

[a] Using the joule effect instead of the oven.

fibers. To generate a value-added product, these composites were applied as a coating, exhibiting high electrical conductivity and excellent thermally activated repair capabilities, both in an oven and through the Joule effect with the application of low voltages. It was demonstrated that the intrinsic properties of the developed material could reduce the energy consumption for its own generation of heating for self-healing,

The study revealed that highly electrically conductive materials (up to 16.50 S/m) can be achieved using mechanically recycled carbon fibers as reinforcement in an insulating epoxy resin. This performance surpasses most common contents of carbon nanoparticles and achieved without thermal or chemical treatments, representing a fourfold increase in electrical conductivity (from 4.03 to 16.50 S/m). It is also important to note the negative impact of the PCL content on electrical conductivity, a behavior noted in previous studies that warrants further investigation for optimization.

An epoxy/PCL matrix was successfully reinforced with recycled carbon fibers to produce a coating with self-healing capabilities activated by Joule effect heating. This novel epoxy/PCL/rCF coating achieved healing efficiencies of 80–90% for surface cracks by applying only 20 V, resulting in a 99% more efficient energy consumption compared to oven heating. The voltage required to reach the set temperature and induce self-healing was reduced by 90% (from 200 V to 20 V) compared to existing literature. Future research should focus on developing this material further to characterize self-healing of internal cracks and evaluate mechanical properties.

Finally, the development of this new type of smart coating holds potential applications in aviation, particularly for anti-icing, the self-healing capability of the coating reducing maintenance, extend the end-of-life (EoL) of engines and thus promoting a circular economy. Another non-industrial application could be as a floor coating in private homes to produce heat via floor radiation, with temperature control through applied voltage, resulting in energy savings.

CRediT authorship contribution statement

Emma Espeute: Writing – review & editing, Writing – original draft, Visualization, Methodology, Investigation, Formal analysis, Data curation, Conceptualization. **David Martinez-Diaz:** Writing – review & editing, Visualization, Methodology, Investigation, Formal analysis, Data curation, Conceptualization. **Pablo Vázquez Sánchez:** Writing – review & editing, Validation, Resources. **Zulima Martín:** Writing – review & editing, Validation, Resources. **Gilberto Del Rosario:** Methodology. **Alberto Jiménez-Suárez:** Writing – review & editing, Validation, Supervision, Methodology. **Silvia G. Prolongo:** Writing – review & editing, Validation, Supervision, Methodology.

Declaration of competing interest

The authors declare that they have no known competing financial interests or personal relationships that could have appeared to influence the work reported in this paper.

Data availability

Data will be made available on request.

Acknowledgements

This work was supported by the project TED2021-131102B-C21, funded by MCIN/AEI/10.13039/501100011033 and the European Union "NextGenerationEU"/PRTR; and the project PID2022-138496OB-I00 from Agencia Estatal de Investigación of Spanish Government and AIRBUS OPERATIONS S.L. inside the activity "EOL SELF-HEALING COATING" funded by "Centro para el Desarrollo Tecnológico y la Innovación" (CDTI) in the project EXP 00152441/IDI-20230293 with the patent application number EP 23382981.1.

References

A. Bellam Balaji, C. Rudd, X. Liu, Recycled Carbon Fibers (rCF) in Automobiles: Towards Circular Economy, (n.d.). https://doi.org/10.1007/s42824-020-00004-0/Published.

Bhandari, M., Nam, I.W., 2024. A critical review on the application of recycled carbon fiber to concrete and cement composites. Recycling 9. https://doi.org/10.3390/recycling9010017.

Bianchi, I., Forcellese, A., Marconi, M., Simoncini, M., Vita, A., Castorani, V., 2021. Environmental impact assessment of zero waste approach for carbon fiber prepreg scraps. Sustainable Materials and Technologies 29, e00308. https://doi.org/10.1016/J.SUSMAT.2021.E00308.

Böhringer, C., 2003. The kyoto protocol: a review and perspectives. https://academic.oup.com/oxrep/article/19/3/451/440601.

Chapman, L., 2007. Transport and climate change: a review. J. Transport Geogr. 15, 354–367. https://doi.org/10.1016/j.jtrangeo.2006.11.008.

Chen, J., Han, J., Xu, D., 2019. Thermal and electrical properties of the epoxy nanocomposites reinforced with purified carbon nanotubes. Mater. Lett. 246, 20–23. https://doi.org/10.1016/J.MATLET.2019.03.037.

Chen, C.H., Chiang, C.L., Wang, J.X., Shen, M.Y., 2022. A circular economy study on the characterization and thermal properties of thermoplastic composite created using regenerated carbon fiber recycled from waste thermoset CFRP bicycle part as reinforcement. Compos. Sci. Technol. 230, 109761 https://doi.org/10.1016/J.COMPSCITECH.2022.109761.

Cheng, H., Guo, L., Zheng, L., Qian, Z., Su, S., 2022. A closed-loop recycling process for carbon fiber-reinforced polymer waste using thermally activated oxide semiconductors: carbon fiber recycling, characterization and life cycle assessment. Waste Manag. 153, 283–292. https://doi.org/10.1016/J.WASMAN.2022.09.008.

Dayi, O., Afsharzadeh, A., Mascle, C., 2016. A Lean based process planning for aircraft disassembly. IFAC-PapersOnLine 49, 54–59. https://doi.org/10.1016/J.IFACOL.2016.03.010.

El-Tantawy, F., Kamada, K., Ohnabe, H., 2002. In situ network structure, electrical and thermal properties of conductive epoxy resin–carbon black composites for electrical heater applications. Mater. Lett. 56, 112–126. https://doi.org/10.1016/S0167-577X(02)00401-9.

Gharfalkar, M., Court, R., Campbell, C., Ali, Z., Hillier, G., 2015. Analysis of waste hierarchy in the European waste directive 2008/98/EC. Waste Manag. 39, 305–313. https://doi.org/10.1016/J.WASMAN.2015.02.007.

Hagnell, M.K., Åkermo, M., 2019. The economic and mechanical potential of closed loop material usage and recycling of fibre-reinforced composite materials. J. Clean. Prod. 223, 957–968. https://doi.org/10.1016/J.JCLEPRO.2019.03.156.

Imran, K.A., Shivakumar, K.N., 2018. Enhancement of electrical conductivity of epoxy using graphene and determination of their thermo-mechanical properties. J. Reinforc. Plast. Compos. 37, 118–133. https://doi.org/10.1177/0731684417736143.

Jiménez-Suárez, A., Del Rosario, G., Sánchez-Romate, X.X., Prolongo, S.G., 2020. Influence of morphology on the healing mechanism of PCL/epoxy blends. Materials 13. https://doi.org/10.3390/MA13081941.

Karuppannan Gopalraj, S., Kärki, T., 2020. A review on the recycling of waste carbon fibre/glass fibre-reinforced composites: fibre recovery, properties and life-cycle analysis. SN Appl. Sci. 2 https://doi.org/10.1007/s42452-020-2195-4.

Keith, M., Leeke, G.A., Keith, M.J., Oliveux, G., 2016. Optimisation of solvolysis for recycling carbon fibre reinforced composites. https://www.researchgate.net/publication/305043711.

Knappich, F., Klotz, M., Schlummer, M., Wölling, J., Mäurer, A., 2019. Recycling process for carbon fiber reinforced plastics with polyamide 6, polyurethane and epoxy matrix by gentle solvent treatment. Waste Manag. 85, 73–81. https://doi.org/10.1016/J.WASMAN.2018.12.016.

Lee, M., Kim, D.H., Park, J.J., You, N.H., Goh, M., 2020. Fast chemical recycling of carbon fiber reinforced plastic at ambient pressure using an aqueous solvent accelerated by a surfactant. Waste Manag. 118, 190–196. https://doi.org/10.1016/J.WASMAN.2020.08.014.

Li, X., Bai, R., McKechnie, J., 2016. Environmental and financial performance of mechanical recycling of carbon fibre reinforced polymers and comparison with conventional disposal routes. J. Clean. Prod. 127, 451–460. https://doi.org/10.1016/J.JCLEPRO.2016.03.139.

Lopez-Urionabarrenechea, A., Gastelu, N., Acha, E., Caballero, B.M., de Marco, I., 2021. Production of hydrogen-rich gases in the recycling process of residual carbon fiber reinforced polymers by pyrolysis. Waste Manag. 128, 73–82. https://doi.org/10.1016/J.WASMAN.2021.04.044.

Luo, X., Ou, R., Eberly, D.E., Singhal, A., Viratyaporn, W., Mather, P.T., 2009. A thermoplastic/thermoset blend exhibiting thermal mending and reversible adhesion. ACS Appl. Mater. Interfaces 1, 612–620. https://doi.org/10.1021/am8001605.

Luo, X., Lauber, K.E., Mather, P.T., 2010. A thermally responsive, rigid, and reversible adhesive. Polymer (Guildf) 51, 1169–1175. https://doi.org/10.1016/j.polymer.2010.01.006.

Martinez-Diaz, D., Cortés, A., Jiménez-Suárez, A., Prolongo, S.G., 2022. Hardener isomerism and content of dynamic disulfide bond effect on chemical recycling of epoxy networks. ACS Appl. Polym. Mater. 4, 5068–5076. https://doi.org/10.1021/acsapm.2c00598.

Martinez-Diaz, D., Espeute, E., Jiménez-Suárez, A., Prolongo, S.G., 2023. Electrical and joule heating capabilities of multifunctional coatings based on recycled carbon fiber from prepreg scrap. ACS Omega 8, 46548–46559. https://doi.org/10.1021/acsomega.3c05413.

Moghaddam, S.M., Nazari, M.R., Soufizadeh, S., 2018. Integrating ecological impact indicators into economic restructuring decisions. Ecol. Indicat. 89, 327–335. https://doi.org/10.1016/j.ecolind.2018.01.045.

Pal, G., Kumar, S., 2016. Multiscale modeling of effective electrical conductivity of short carbon fiber-carbon nanotube-polymer matrix hybrid composites. Mater. Des. 89, 129–136. https://doi.org/10.1016/j.matdes.2015.09.105.

Pimenta, S., Pinho, S.T., 2011. Recycling carbon fibre reinforced polymers for structural applications: technology review and market outlook. Waste Manag. 31, 378–392. https://doi.org/10.1016/J.WASMAN.2010.09.019.

Polymer Blend Nanocomposites for Energy Storage Applications, 2023. Elsevier. https://doi.org/10.1016/C2021-0-01800-9.

Prolongo, S.G., Moriche, R., Del Rosario, G., Jiménez-Suárez, A., Prolongo, M.G., Ureña, A., 2016. Joule effect self-heating of epoxy composites reinforced with graphitic nanofillers. J. Polym. Res. 23 https://doi.org/10.1007/s10965-016-1092-4.

Raji, A.R.O., Varadhachary, T., Nan, K., Wang, T., Lin, J., Ji, Y., Genorio, B., Zhu, Y., Kittrell, C., Tour, J.M., 2016. Composites of graphene nanoribbon stacks and epoxy for joule heating and deicing of surfaces. ACS Appl. Mater. Interfaces 8, 3551–3556. https://doi.org/10.1021/acsami.5b11131.

Ran, Hongyu, Elchalakani, Mohamed, Yehia, Sherif, Ali Sadakkathulla, Mohamed, Guo, Xiao, 2024. Mechanical, electrical and self-healing properties of carbon fibre-reinforced ultra-lightweight ECC. J. Build. Eng. 84 https://doi.org/10.1016/j.jobe.2024.108513.

Saberi, M., Ansari, R., Hassanzadeh-Aghdam, M.K., 2023. Predicting the electrical conductivity of short carbon fiber/graphene nanoplatelet/polymer composites. Mater. Chem. Phys. 309 https://doi.org/10.1016/j.matchemphys.2023.128324.

Sánchez-Romate, X.F., Sans, A., Jiménez-Suárez, A., Campo, M., Ureña, A., Prolongo, S. G., 2020a. Highly multifunctional gnp/epoxy nanocomposites: from strain-sensing to joule heating applications. Nanomaterials 10, 1–15. https://doi.org/10.3390/nano10122431.

Sánchez-Romate, X.F., Martín, J., Jiménez-Suárez, A., Prolongo, S.G., Ureña, A., 2020b. Mechanical and strain sensing properties of carbon nanotube reinforced epoxy/poly (caprolactone) blends. Polymer (Guildf) 190. https://doi.org/10.1016/j.polymer.2020.122236.

Sánchez-Romate, X.F., Sans, A., Jiménez-Suárez, A., Prolongo, S.G., 2021. The addition of graphene nanoplatelets into epoxy/polycaprolactone composites for autonomous self-healing activation by Joule's heating effect. Compos. Sci. Technol. 213 https://doi.org/10.1016/j.compscitech.2021.108950.

Sánchez-Romate, X.F., González, C., Jiménez-Suárez, A., Prolongo, S.G., 2022. Novel approach for damage detection in multiscale CNT-reinforced composites via wireless Joule heating monitoring. Compos. Sci. Technol. 227 https://doi.org/10.1016/j.compscitech.2022.109614.

Sangroniz, L., Landa, M., Fernández, M., Santamaria, A., 2021. Matching rheology, conductivity and joule effect in PU/CNT nanocomposites. Polymers 13. https://doi.org/10.3390/polym13060950.

Shuaib, N.A., Mativenga, P.T., 2016. Energy demand in mechanical recycling of glass fibre reinforced thermoset plastic composites. J. Clean. Prod. 120, 198–206. https://doi.org/10.1016/J.JCLEPRO.2016.01.070.

Simonini, L., Mahmood, H., Dorigato, A., Pegoretti, A., 2023. Evaluation of self-healing capability of a polycaprolactone interphase in epoxy/glass composites. Compos Part A Appl Sci Manuf 169. https://doi.org/10.1016/j.compositesa.2023.107539.

Sommer, V., Walther, G., 2021. Recycling and recovery infrastructures for glass and carbon fiber reinforced plastic waste from wind energy industry: a European case study. Waste Manag. 121, 265–275. https://doi.org/10.1016/J.WASMAN.2020.12.021.

Stefan, Gossling, Paul, Upham, 2009. Climate change and aviation, london. https://doi.org/10.4324/9781849770774.

Sukanto, H., Raharjo, W.W., Ariawan, D., Triyono, J., 2021. Carbon fibers recovery from CFRP recycling process and their usage: a review. IOP Conf. Ser. Mater. Sci. Eng. 1034, 012087 https://doi.org/10.1088/1757-899X/1034/1/012087.

Taherian, R., Ghorbani, M.M., 2017. Investigation of the electrical properties of polymer/carbon composites exposed to joule heating and heat treatment. ECS Journal of Solid State Science and Technology 6, M3019–M3027. https://doi.org/10.1149/2.0051706jss.

Tsotra, P., Friedrich, K., 2004. Short carbon fiber reinforced epoxy resin/polyaniline blends: their electrical and mechanical properties. Compos. Sci. Technol. 64, 2385–2391. https://doi.org/10.1016/j.compscitech.2004.05.003.

Vo Dong, P.A., Azzaro-Pantel, C., Cadene, A.L., 2018. Economic and environmental assessment of recovery and disposal pathways for CFRP waste management. Resour. Conserv. Recycl. 133, 63–75. https://doi.org/10.1016/j.resconrec.2018.01.024.

Wang, C.H., Duong, C.N., 2016. Introduction and overview. In: Bonded Joints and Repairs to Composite Airframe Structures. Elsevier, pp. 3–19. https://doi.org/10.1016/B978-0-12-417153-4.00001-3.

Wang, Y., Li, A.Y., Zhang, S.H., Guo, B.B., Niu, D.T., 2023. A review on new methods of recycling waste carbon fiber and its application in construction and industry. Construct. Build. Mater. 367 https://doi.org/10.1016/j.conbuildmat.2023.130301.

White, S.R., Mather, P.T., Smith, M.J., 2002. Characterization of the cure-state of DGEBA-DDS epoxy using ultrasonic, dynamic mechanical, and thermal probes. Polym. Eng. Sci. 42, 51–67. https://doi.org/10.1002/pen.10927.

Witik, R.A., Teuscher, R., Michaud, V., Ludwig, C., Månson, J.A.E., 2013. Carbon fibre reinforced composite waste: an environmental assessment of recycling, energy recovery and landfilling. Compos Part A Appl Sci Manuf 49, 89–99. https://doi.org/10.1016/j.compositesa.2013.02.009.

Wu, J., Gao, X., Wu, Y., Wang, Y., Nguyen, T.T., Guo, M., 2023. Recycling carbon fiber from carbon fiber-reinforced polymer and its reuse in photocatalysis: a review. Polymers 15. https://doi.org/10.3390/polym15010170.

Xu, X., Zhao, X., Vokhidova, N.R., Sun, Q., Li, Y., Lu, Y., 2023. Aircraft coating for electromagnetic interference shielding with flame retardancy and Joule heating capability. Mater. Chem. Phys. 299 https://doi.org/10.1016/j.matchemphys.2023.127539.

Zhang, J., Chevali, V.S., Wang, H., Wang, C.H., 2020. Current status of carbon fibre and carbon fibre composites recycling. Compos. B Eng. 193 https://doi.org/10.1016/j.compositesb.2020.108053.

Zhao, Y., Liu, H., Li, S., Chen, P., Jiang, S., Liu, J., Meng, F., 2022. Rapid joule-heating activation boosted capacitive performance of carbon fibers. Compos. Commun. 34, 101263 https://doi.org/10.1016/J.COCO.2022.101263.

Zhao, X., Long, Y., Xu, S., Liu, X., Chen, L., Wang, Y.Z., 2023. Recovery of epoxy thermosets and their composites. Mater. Today 64, 72–97. https://doi.org/10.1016/J.MATTOD.2022.12.005.